Linking LIDAR with streamwater biogeochemistry in coastal temperate rainforest watersheds

Jason B. Fellman*
Environmental Science Program and Alaska Coastal Rainforest Center
University of Alaska Southeast, Juneau, AK 99801
Email: jbfellman@uas.alaska.edu

Brian Buma
Environmental Science Program, University of Alaska Southeast, Juneau, AK 99801
Email: bbuma@uas.alaska.edu

Eran Hood
Environmental Science Program, University of Alaska Southeast, Juneau, AK 99801
Email: ewhood@uas.alaska.edu

Richard T. Edwards
U.S.D.A. Forest Service, Pacific Northwest Research Station, Juneau, Alaska 99801
Email: rtedwards@fs.fed.us

David V. D'Amore
U.S.D.A. Forest Service, Pacific Northwest Research Station, Juneau, Alaska 99801
Email: ddamore@fs.fed.us

*Corresponding author:
Jason Fellman
Environmental Science Program and Alaska Coastal Rainforest Center
University of Alaska Southeast
Juneau, AK 99801
Fax: 907-796-6406
Telephone: 907-796-6370
Email: jbfellman@uas.alaska.edu

Abstract

The goal of this study was to use watershed characteristics derived from LIDAR data to predict stream biogeochemistry in Pacific coastal temperate rainforest (PCTR) watersheds. Over a two-day period, we sampled 37 streams for concentrations of dissolved C, N, P, major cations and measures of dissolved organic matter (DOM) quality (specific ultraviolet absorbance, $SUVA_{254}$) and bioavailability. Random forest/classification tree (CART) analysis showed that aboveground biomass and structure and watershed characteristics, inclusive of mean watershed slope and elevation, watershed size and topographic wetness, explained more than 60% of the variation in concentration for most measured constituents. These results indicate this approach may be particularly useful for predicting stream biogeochemistry in small forested watersheds where fine resolution is needed to resolve subtle differences in forest biomass, structure and topography. Overall, we suggest that the use of LiDAR in many of the small and remote watersheds across the southeast Alaskan PCTR as well as other forested regions could help inform land management decisions that have the potential to alter ecosystems services related to watershed biogeochemical fluxes.

Key Words: stream biogeochemistry, LIDAR, dissolved organic matter, stable water isotopes

Introduction

Stream export of terrestrial-derived dissolved organic matter (DOM) is increasingly being recognized as an important component of watershed-scale carbon cycling because of impacts to the carbon balance of terrestrial ecosystems, especially over decadal time scales (Cole et al. 2007). Riverine DOM also acts as a vector for nitrogen (N), phosphorus (P), trace metals and contaminants (Qualls and Richardson 2003, Pellerin et al. 2004, Lidman et al. 2014) making the terrestrial-aquatic flux of DOM an important control on the ecology (e.g., heterotrophic metabolism) and chemical properties (e.g., pH) of aquatic ecosystems (Dalzell et al. 2005, Wiegner et al. 2005). These ecological qualities of DOM vary with its chemical quality and bioavailability. Hence, DOM derived from different watershed sources (e.g., urban runoff, wetland and forest soils) may have different impacts on aquatic ecosystem processes (Kaplan and Bott 1985, Williams et al. 2010).

Streamwater DOM, measured as dissolved organic carbon (DOC), and nutrient concentrations (N and P) are controlled by multiple watershed characteristics including landscape/soil type, land-use history, watershed size and vegetation (Clark et al. 2004, Kaplan et al. 2006, Tank et al. 2012). Wetlands are a well-recognized source of DOM and nutrients to streams and many studies have used watershed wetland coverage as a first order approximation of DOC concentrations (Dillon and Molot 1997, Gergel et al. 1999, D'Amore et al. 2015). However, wetland coverage alone cannot predict the spatial and temporal variability in streamwater DOM (Ågren et al. 2007). This is particularly true as watersheds increase in size and complexity, and as varying ecological factors (e.g., species composition, cover type) influence the availability of soluble DOM for export to streams. Moreover, streamwater DOM and nutrient fluxes are being altered in many regions as a result of forest conversion (Stanley and

Maxted 2008, Moore et al. 2013, Regnier et al. 2013) urban development (Pellerin et al. 2004, Petrone 2010) and hydrologic modification (Miller 2012). Thus, quantifying DOM and nutrient export from varied landscape types helps elucidate how topography, biological factors (e.g. aboveground biomass) and land use change impact stream carbon export.

There has been much research over the last several decades attempting to relate landscape characteristics to stream biogeochemistry (Dillon and Molot 1997, Mattsson et al. 2005, Stanley and Maxted 2008). Yet, many of these landscape analyses have had mixed success in predicting stream biogeochemical concentrations (Frost et al. 2006, Cuevas et al. 2006). Thus, new tools for predicting streamwater biogeochemistry at the watershed-scale are necessary, particularly for improving land management as it pertains to biogeochemical cycling. LiDAR (light detection and ranging) is a remote sensing technology commonly used to acquire topography of the ground surface (bare earth) and vegetation structure (surface model) at fine spatial resolution over large scales. Recent research has highlighted the ability of LiDAR to model forest biomass, structure and composition (Hudak et al. 2012). LiDAR has also been useful for estimating DOC concentrations in boreal forest streams using contributing landscape components because it provides a robust level of detail for watershed characteristics such as slope and watershed surface area (Creed et al. 2008, Ågren et al. 2014). Being able to use LIDAR as a predictive tool would be especially beneficial in heterogeneous landscapes such as the Perhumid Coastal Temperate Rainforest (PCTR) of southeast Alaska where small headwater streams are abundant, poorly accessible for sampling and estimated to contain some of the highest areal DOC fluxes in the world (D'Amore et al. 2015).

The goal of this study was to use watershed landcover characteristics derived from LIDAR data, such as biomass, watershed morphology and relative disturbance exposure, to

predict stream biogeochemistry in PCTR watersheds. Over a two-day period, we sampled 37 streams draining small sub-watersheds and analyzed the surface water for N, P, DOM concentration, quality (as measured by the specific ultraviolet absorbance, $SUVA_{254}$) and bioavailability and major cations. Linking high-resolution forest structural information with stream biogeochemical concentrations is a relatively novel application of LiDAR, which could provide an improved method for estimating the land-to-ocean flux of DOM and nutrients in this region. We also measured stable isotopes of water ($\delta^{18}O$) in all study streams to help identify watershed sources of streamwater and their potential influence on stream biogeochemistry.

Methods

Site description and field methods

Streamwater was collected from the Cowee Creek watershed located on the western margin of the 3800 km^2 Juneau Icefield. The research watershed is part of the USDA Forest Service Héen Latinee Experimental Forest, near Juneau, Alaska (Fig. 1). Juneau has a moderate maritime climate with persistent cloud cover and a mean monthly temperature at sea level ranging from -2 to 14 °C. Numerous glacial epochs have sculpted the Coast Mountains of southeast Alaska leaving steep sloping watersheds with serrated ridges creating an orographic barrier that results in a mean annual precipitation at sea level in Juneau of ~2,100 mm but is estimated to be as high as 5,000 mm at higher elevations. Most of this precipitation falls as rain during large frontal storms in autumn (Aug-Nov) or as snow at high elevations during the winter. Southeast Alaska also contains extensive lowlands containing carbon-rich peatlands mixed with coniferous forest resulting in some of the densest terrestrial carbon stocks (>300 Mg C ha^{-1}) in

the world (Heath et al. 2011). Soil carbon densities in the regions abundant wetlands can be as high as 600 Mg C ha^{-1} (Johnson et al. 2011).

The 118 km^2 Cowee Creek watershed contains three hanging glaciers with 13% of the watershed covered by glacier ice, 57% covered by forest and 5% covered by wetlands (Fellman et al. 2014b). The remainder of the watershed consists of alpine landscapes. Average watershed elevation is 638 m, with a mean slope of 23º. The upper reaches of the watershed are characterized by recently deglaciated terrain with high alpine tundra, exposed bedrock, poorly developed soils and little vascular vegetation. At mid to lower elevations, the landscape is older, consisting of mixed coniferous forest dominated by *Picea sitchensis* and *Tsuga heterophylla* with an understory of blueberry (*Vaccinium* spp.) on moderate slopes and well-drained flat lands and *Alnus* (spp.) along avalanche/landslide paths and riparian areas. In low-gradient areas that are poorly drained, forested and unforested wetlands develop: forested dominated by *P. sitchensis* and *T. heterophylla* with an understory of skunk cabbage (*Lysichiton americanum*) and *Vaccinium* spp., and unforested dominated by Ericaceous shrubs, sedges (*Carex* spp.), shore pine (*Pinus contorta)* and *Sphagnum* spp.

Streamwater was collected from 37 sub-watersheds within the Cowee Creek watershed over a two-day period in July of 2014 (Fig 1). The 37 sub-watersheds range in area from <1.0 to 16.7 km^2 with an average slope of 23.7º (Table 1). Although the lower reaches of Cowee Creek contain anadromous salmon, the small and steeply sloping study streams do not support salmon. Streams were sampled during mid-summer baseflow conditions before the onset of the late summer/early fall wet season in the region. All streamwater samples were field-filtered through pre-combusted (450 ºC for 4 hrs), Whatman glass fiber filters (nominal pore size 0.7 μm) and placed in acid washed polyethylene bottles for nutrient and cation analyses and in pre-combusted

(450 ºC for 4 hrs) glass vials for DOM analyses. Stream temperature and specific conductivity were measured at the study reach using a hand-held YSI (model 556) meter.

Landscape components and LiDAR analysis

LiDAR measurements of Cowee Creek watershed were obtained at an average point density of ~8 measurements per m^2. These data were used to produce a high-resolution 1 m^2 DEM of the watershed, from which sub-watersheds for each of the 37 stream sampling sites were delineated. Mean aboveground biomass, canopy cover percentage and tree height were extracted from the LiDAR map (details below). The mean slope, percent of the area less than 10º slope, mean watershed elevation, watershed area, watershed surface area and topographic wetness index (TWI, indicator of soil moisture conditions and is calculated using the upslope contributing area and slope, Sørensen et al. 2006) were extracted from the LiDAR DEM. Finally, mean wind exposure (calculated based on topographic sheltering from predominant storm tracks in the region) and slide suitability (susceptibility to landslide initiation and is based on topographic drivers such as slope and topographic position) were calculated from LIDAR data following (Buma and Johnson 2015). The end result is a suite of vegetative, topographic, and disturbance-relevant variables describing each sub-watershed.

Determination of aboveground biomass

Aboveground biomass was mapped using high resolution LiDAR. Extensive field biomass measurements were completed to calibrate the watershed biomass map. Briefly, 47 plots (400 m^2) were established throughout the study area, stratified according to observed canopy height (utilizing a preliminary 5x5m LiDAR map) so the entire range of aboveground biomass was sampled. At each point, all trees were measured for species, diameter at breast height, canopy condition, breakage, and live/dead status. Total standing aboveground biomass was then

178 tallied using equations from Ter-Mikaelian and Korzukhin (1997) and Standish et al. (1985). For
179 broken trees, actual height was estimated using (Keyser 2008) and then tapering equations from
180 (Kozak et al. 1969) were applied to generate accurate biomass estimates. Foliage mass was
181 removed from dead trees; if tree species could not be determined it was assumed to be *P.*
182 *sitchensis* for biomass calculations. Standing biomass was assumed to be 50% carbon. For
183 downed material, the standard line-intercept method of Brown (1974) was used. Two 20m
184 perpendicular lines were measured for each plot. A specific gravity of 0.39 and 0.19 for sound
185 and rotten wood was assumed for carbon calculations (Harmon et al. 2011). The total carbon at
186 each point was then modeled from the LiDAR data using standard methods (e.g., Hudak et al.
187 2012). Briefly, using a multivariate adaptive regression splines technique (Friedman 1991,
188 Güneralp et al. 2014), 61 statistical descriptions of the LiDAR point cloud (e.g., median height of
189 all returns, 20m resolution), and 5 additional spatial datasets (forest type, land cover,
190 precipitation, wind exposure, and landslide susceptibility), observed biomass was fit to the
191 LiDAR data and then extrapolated over the entire watershed. The final model was a good fit to
192 the observed data without overfitting ($r^2 = 0.76$, mean error 2.03 Mg/ha). The result is a 20 m
193 resolution biomass map of the entire study area (see Hudak et al. 2012 for full details).
194 *Biogeochemical and stable water isotope analyses*
195 A 25 ml water sample was also collected for $\delta^{18}O$ analysis of streamwater to assist in
196 identification of the different water sources (e.g., rainwater vs. snowmelt) contributing to
197 streamflow. Snow and glacier ice are often depleted in $\delta^{18}O$ relative to rainfall and groundwater
198 because low temperatures and increasing elevation typically result in natural fractionation
199 (Dansgaard 1964, Dietermann and Weiler 2013). Thus, comparison of $\delta^{18}O$ in precipitation and
200 surface water can be used for flow path analysis and runoff generation (Vitvar and Balderer

1997) and as an indicator of the origin of surface water in watersheds where glacier ice and snowmelt contribute to streamflow (Fellman et al. 2014a). Water isotope samples were stored in glass bottles with zero headspace at room temperature until analysis on a Picarro L2120-i analyzer. Values for $\delta^{18}O$ are reported in per mil (‰) after normalization to Vienna standard mean ocean water (VSMOW, Paul et al. 2007).

Concentrations of DOC and total dissolved N (TDN) were analyzed by high temperature combustion (non-purgeable organic carbon) on a Shimadzu TOC-V-CSH analyzer using a high sensitivity catalyst to enable low detection limits for DOC. Analytical precision for DOC ranged from 0.02-0.04 mg C L^{-1} for concentrations less than 5 mg C L^{-1} and 0.1-0.2 mg C L^{-1} for samples greater than 5 mg C L^{-1}. Major anions (NO_3-N) were measured using a Dionex DX600 ion chromatograph with an AS18A anion column and cations (Ca, K, Mg and NH_4-N) were measured using a Dionex ICS-1500 with a CS16C cation column. Dissolved organic nitrogen (DON) was calculated as the difference between TDN and dissolved inorganic N (DIN = NH_4-N + NO_3-N). Soluble reactive phosphorus (SRP) was measured using the ascorbic acid method (Murphy and Riley 1962) with a 5 cm quartz cell to enable the detection of low SRP concentrations (lower detection limit of ~1 µg P L^{-1}). Total phosphorus (TP) was measured by persulfate digestion combined with the ascorbic acid method (Valderrama 1981).

We used specific ultraviolet absorbance ($SUVA_{254}$) to assess DOM quality (Weishaar et al. 2003). The $SUVA_{254}$ of DOM, which is an indicator of aromatic carbon content, was measured at 254 nm on a Genesys 5 Spectrophotometer. In forested and wetland streams, $SUVA_{254}$ typically ranges from 3 to 5 L mg-C^{-1} m^{-1} corresponding to an aromatic C content of 15–35% (Weishaar et al. 2003). Bioavailable DOC (BDOC) was measured for each stream using laboratory incubations following the methods of Fellman et al. (2008). Streamwater was initially

filtered through a 0.2 µm filter, a microbial inoculum was added, DOC was analyzed and samples were incubated in the dark at room temperature. After 30 days, the solution was re-filtered through a 0.2 µm filter, DOC was re-measured, and BDOC was calculated as the difference in sample DOC before and after the 30-day incubation. The microbial inoculum was prepared by leaching stream sediments followed by filtration through a Whatman GF/D filter (2.7 µm).

Statistical Methods

For each chemical species considered, an identical statistical procedure was followed for analysis. A random forest/classification tree (CART) technique was used. CART models are useful when complex interactions and autocorrelation between variables are expected (Brieman et al. 1984), data are often non-normally distributed, and interpretable results are needed (as opposed to simply a predictive model). However, it is susceptible to non-optimal solutions and as a result, variable selection prior is often practiced (e.g. (Cutler et al. 2007). In this case, the five most important variables (as measured by total reduction in deviance) were determined using Random Forest (Brieman 2001). While this method is robust to the non-optimal solutions, interpreting interactions between the variables is difficult. To investigate specific interactions between those variables, traditional CART methods using the rpart package from R were utilized. Optimal tree size was determined by minimizing the 10-fold cross validated error. Linear regressions in R were calculated where appropriate and if necessary, data were log transformed to meet normality and equal variance assumptions.

Results

Water $\delta^{18}O$ analysis

247 Streamwater $\delta^{18}O$ values ranged from -10.2‰ to -14.4‰, with an average of -12.5‰
248 (Table 1, Fig. 2). These values were slightly more depleted than the mean value for historical
249 rainfall (-11.7‰, Fellman et al. 2014) collected in Juneau (~60 km southeast of Cowee Creek)
250 likely indicating isotopically depleted water from snowmelt contributed to streamflow in a
251 number of our study streams. Regression analyses showed that as watershed size ($r^2 = 0.27$, $P <$
252 0.01, $\log_{10}$ transformed), max elevation ($r^2 = 0.23$, $P < 0.01$, $\log_{10}$ transformed) and mean
253 watershed slope increased ($r^2 = 0.48$, $P < 0.01$, $\log_{10}$ transformed), streamwater $\delta^{18}O$ values
254 become more depleted. The random forest/CART analysis (model $r^2 = 0.81$) identified mean
255 watershed slope followed by the percentage of the watershed <10º as the most useful in
256 explaining streamwater $\delta^{18}O$ values (Fig. 2).

257 *Dissolved organic matter concentration, quality and bioavailability*

258 Concentrations of DOC ranged from 0.6 to 30.5 mg C L^{-1} across the study streams but
259 only four streams had concentrations >10.0 mg C L^{-1} (Table 1, Fig. 3a). Random forest/CART
260 analysis identified four landscape components that explained the greatest variation in stream
261 DOC concentration (model $r^2 = 0.89$), with mean watershed slope (negative relationship) the
262 strongest predictor of DOC (Fig. 3a). In watersheds with a mean slope >13.75º (n=34),
263 aboveground biomass (negative relationship) and to a lesser extent topographic wetness and % of
264 low-slope area (<10º) best explained stream DOC concentration (Fig. 3a). Similar to DOC, mean
265 watershed slope (negative relationship) was the strongest predictor of streamwater DON
266 concentration (model $r^2 = 0.80$, Fig. 3b). Mean tree height (negative relationship) was also
267 associated with low streamwater DON concentration in high gradient watersheds (slope
268 ≥15.25º). Overall, concentrations of DOC and DON were positively related for all streams

269 together ($r^2 = 0.81$, $P < 0.01$, $\log_{10}$ transformed) and negatively related to streamwater $\delta^{18}O$
270 values (DOC $r^2 = 0.47$, $P < 0.01$, DON $r^2 = 0.47$, $P < 0.01$).

271 Streamwater $SUVA_{254}$ values varied from 3.0 to 4.7 L mg C^{-1} m^{-1} across the study
272 streams (Table 1), corresponding to a range in aromaticity of 23 to 34% (Weishaar et al. 2003).
273 Random forest/CART analysis showed that landslide susceptibility (negative relationship) was
274 the strongest predictor of $SUVA_{254}$ values (model $r^2 = 0.77$, Fig. 4a). In watersheds with low
275 landslide susceptibility, mean slope (negative relationship) was the strongest predictor of
276 $SUVA_{254}$ values followed by landslide susceptibility (on that subset of plots) and aboveground
277 biomass (Fig. 4a). Overall, $SUVA_{254}$ values were negatively related to landslide susceptibility (r^2
278 $= 0.35$, $p < 0.01$) and positively related to streamwater $\delta^{18}O$ values ($r^2 = 0.34$, $P < 0.01$) across all
279 streams.

280 Percent BDOC varied from 3 to 28% (0.1 to 5.0 mg C L^{-1}) across the study streams.
281 Random forest/CART analysis identified four predictor variables that best explained streamwater
282 BDOC concentration (model $r^2 = 0.93$, Fig. 4b), with mean watershed slope (negative
283 relationship) the strongest predictor of concentrations ($r^2 = 0.28$, $P < 0.01$, $\log_{10}$ transformed).
284 Topographic wetness (positive relationship) was also important in controlling BDOC
285 concentration in low gradient watersheds whereas aboveground biomass and mean watershed
286 elevation were important in steeply sloping watersheds. Concentrations of BDOC were
287 positively related to $SUVA_{254}$ values ($r^2 = 0.43$, $P <0.01$, $\log_{10}$ transformed) and SRP
288 concentrations ($r^2 = 0.18$, $P < 0.01$, $\log_{10}$ transformed), providing evidence of a link between
289 DOM quality, nutrient availability and DOC bioavailability to stream microbial communities.
290 Similar to DOM concentration, $\delta^{18}O$ values were positively related to $SUVA_{254}$ ($r^2 = 0.34$, $P <$
291 0.01) and BDOC concentrations ($r^2 = 0.55$, $P < 0.01$, $\log_{10}$ transformed).

292 *Inorganic nutrient concentrations*

293 Concentrations of SRP ranged from below detection to 17.4 µg P L^{-1} (mean of 1.9 µg P
294 L^{-1}) although there were only two streams with concentrations >5 µg P L^{-1} (Table 1, Fig. 5a).
295 Watershed surface area (positive relationship) was the strongest control on streamwater SRP
296 concentration and to a lesser extent slope and landslide exposure (model $r^2 = 0.57$, Fig. 5a).
297 However, cross validation of the model was poor due to the large number of streams with
298 concentrations at or below the lower detection limit (~1 µg P L^{-1}). Mean TP concentrations were
299 19.7 µg P L^{-1}, suggesting inorganic P contributes very little to streamwater P in most of our study
300 streams. Watershed size (positive relationship) explained the most variation in TP concentration
301 (model $r^2 = 0.61$, Fig. 5b), with wind storm exposure and to a lesser extent watershed slope
302 influential in small watersheds (<0.36 km^2). Streamwater DIN concentrations (NO_3-N is ~70%
303 of DIN) were controlled by both landscape and vegetative factors, with mean watershed
304 elevation (negative relationship) the most influential followed by topographic wetness and mean
305 tree height (model $r^2 = 0.66$, Fig. 6). Similar to SRP, DIN concentrations were typically at or
306 near the lower detection limit resulting in poor cross validation of the model.

307 Random forest/CART analysis of streamwater base nutrient cations (Ca^{2+}, Mg^{2+} and K^+)
308 showed that watershed morphology (watershed size and topographic wetness) was the strongest
309 predictor of Ca concentration (model $r^2 = 0.57$, Fig 7). Forest biomass and structure were the
310 most influential controls on K and Mg concentrations. In particular, canopy coverage (positive
311 relationship) controlled K concentration (model $r^2 = 0.74$, Fig. 8a) and aboveground biomass
312 (positive relationship) was surprisingly the most important driver of Mg concentration (model r^2
313 = 0.32, Fig. 8b). Although aboveground biomass was excluded by the CART analysis in favor of

mean canopy cover, these two variables were positively related ($r^2 = 0.93$, $P < 0.01$). Together, these results provide more evidence of a tight vegetative control on streamwater K concentration.

Discussion

Our initial goal of evaluating whether LIDAR generated data on forest biomass, structure, and watershed morphology would be a strong predictor of stream biogeochemistry was supported for most of the biogeochemical species examined in this study. Small, steep streams in the PCTR generally have short water residence times and demonstrate tight hydro-biogeochemical connectivity with terrestrial ecosystems (Fellman et al. 2009, D'Amore et al. 2010). Thus, our approach of sampling numerous small watersheds (mean size <0.5 km^2) minimizes some potential confounding factors, such as the instream uptake and/or production of DOM and nutrients along the stream network (Brookshire et al. 2005, del Giorgio and Pace 2008). We also recognize that sampling streams only once limited our interpretation to the measurement period and this snapshot may miss seasonal changes in underlying drivers of stream biogeochemistry. With these limitations in mind, our findings demonstrate that landscape and vegetative predictors generated from high resolution LIDAR data have clear potential to enhance our understanding of how changes in management regime impact stream biogeochemistry in small to mid-sized forested watersheds.

Our finding that mean watershed slope was the strongest predictor of DOC and DON concentration is consistent with studies in southeast Alaska (D'Amore et al. 2015) and other forested regions (Rasmussen et al. 1989, Frost et al. 2006, Jankowski et al. 2014). This relationship reflects the rapid movement of water and the existence of shallow organic-rich soils in steeper sloped watersheds as opposed to the presence of carbon-rich wetlands in low gradient

watersheds that contribute abundant DOM to streams (Fellman et al. 2009, D'Amore et al. 2010). Wetlands are most common in flatter areas of the watershed, although they can occur on benches in otherwise steeply sloping watersheds or on slopes as steep as 15º in southeast Alaska (D'Amore et al. 2015). Moreover, our finding that in addition to slope, aboveground biomass and to a lesser extent topographic wetness (wetter areas are more likely to contain carbon-rich soils) explained 88% of the variation in stream DOC concentration suggests that LIDAR generated data on forest biomass and watershed morphology is a robust technique for estimating stream DOC. This approach may be particularly useful for predicting stream DOC in small forested watersheds where fine resolution is needed to resolve subtle differences in forest biomass, structure and topography.

Watershed morphology appears to be an important control on stream DOM biogeochemistry, with DOM bioavailability best explained by watershed slope and DOM quality (estimated by $SUVA_{254}$) controlled by landslide susceptibility and watershed slope. The highest BDOC concentrations were associated with low-gradient watersheds, thus confirming the importance of wetlands and/or organic carbon-rich soils as a potential source of bioavailable DOM to stream ecosystems (Kaplan et al. 2006, Fellman et al. 2008). Similarly, DOM derived from wetlands or from forest floors with deep organic soils is enriched in aromatic carbon content (typically $SUVA_{254}$ values 4 to 4.6 L mg-C^{-1} m^{-1}) and typically dominates the DOM pool in low-gradient watersheds (Fellman et al. 2009, Hanley et al. 2013). On the other hand, we hypothesize that in steeply sloping watersheds with high potential for landslide initiation, shallow organic carbon-rich soils combined with DOM adsorption on mineral soils (Qualls and Haines 1992, Qualls 2000) reduces aromatic carbon inputs to streams resulting in $SUVA_{254}$ values generally <4.0 L mg-C^{-1} m^{-1}.

Our findings that streamwater SRP and TP concentrations were best explained by watershed surface area/size, slope, elevation and windstorm exposure was not surprising given landscape erosion can significantly increase the supply of available P to ecosystems (Vitousek et al. 2003, Porder et al. 2005). This combination of predictive variables also suggests exposure to ecological disturbance (i.e. windthrow), which can mix soils and expose material for more rapid weathering, influences streamwater P concentrations. Despite this evidence for weathering of P (mean TP = 19.7 μg P L^{-1}), streamwater SRP concentrations were at or near lower detection (mean = 1.9 μg P L^{-1}) in most of study streams. This suggests efficient retention of available P through biological uptake (Cleveland et al. 2002, Simon et al. 2005, Olander and Vitousek 2005) and sorption of P (Giesler et al. 2004, Olander and Vitousek 2005) in either soils or streams.

The variation in streamwater DIN and base cation concentrations (Mg^{2+}, Ca^{2+} and K^{+}) were best explained by a combination of vegetative and landscape controls across our study watersheds. In particular, streamwater DIN concentrations were elevated in mid to high elevation watersheds with a low to moderate topographic wetness index. This pattern likely results from the leaching of NO_3 from alder (*Alnus* spp.) influenced soils that typically dominate riparian areas and avalanche/landslide paths common to steeply sloping watersheds (Compton et al. 2003). The essential plant nutrients Mg^{2+}, K^{+} and Ca^{2+} are derived from rock weathering and our finding that streamwater Mg^{2+} and K^{+} were best explained by aboveground biomass, canopy coverage and tree height is consistent with the idea that forest productivity (Vitousek 1982) and foliar leaching (Oyarzún et al. 2005) are strong controls on soluble base cation concentrations. However, Ca^{2+} concentrations were mostly strongly related to watershed characteristics (watershed size) suggesting plant uptake and retention was minimal relative to the supply of Ca through rock weathering (Vitousek 1977). Although our findings provide evidence of a

383 vegetative and landscape control on stream Mg, Ca and K, marine aerosols have been shown to
384 influence anion/cation concentrations in coastal streams (Wigington et al. 1998) and therefore
385 provide an additional source of variability not included in our analysis.

386 Streamwater $\delta^{18}O$ values were significantly related to several watershed characteristics
387 (slope, elevation) and stream DOM concentration, bioavailability and $SUVA_{254}$ values. These
388 results are consistent with previous research in the Alaskan PCTR showing that streamwater
389 $\delta^{18}O$ can be used to estimate stream DOM concentration in watersheds where landscape source
390 pools have unique isotopic signatures (Fellman et al. 2014a). Streams with high mean watershed
391 slopes and elevations had the most depleted $\delta^{18}O$ values and lowest DOM concentrations (both
392 DOC and DON) and $SUVA_{254}$ values reflecting the contribution of organic matter poor
393 snowmelt to streamflow. Alternatively, streams with the greatest DOM concentration and most
394 enriched $\delta^{18}O$ values were associated with low-gradient watersheds dominated by wetlands.
395 Moreover, $\delta^{18}O$ values in low-gradient streams were enriched as much as 1.5‰ relative to
396 typical values for historical rainfall in Juneau suggesting water residence time in these
397 watersheds was long enough to allow for evaporative water loss to occur; thus enriching
398 streamwater $\delta^{18}O$ values (Hamilton et al. 2005, Dogramaci et al. 2012). These findings differ
399 from studies of northern forested watersheds (Striegl et al. 2005, Frost et al. 2006), which
400 showed that increased water residence allows for enhanced removal of DOM due to photo and/or
401 biodegradation processes (Lapierre et al. 2013, Kothawala et al. 2014), likely because of the
402 much smaller watershed sizes and lower overall water residence times in our study watersheds.

403 This study demonstrates the usefulness of combining stable isotopes of water and high
404 resolution LIDAR analyses to better understand the dynamics of the streamwater DOM pool. For
405 instance, long term changes in stream DOM export are driven not only by watershed morphology

406 but interacting ecosystem processes such as net ecosystem production, soil carbon and nutrient
407 cycling and watershed hydrology(Evans et al. 2005, Räike et al. 2015, Butman et al. 2016).
408 Understanding the role of varying sources of streamwater in driving watershed DOM export is
409 critical for predicting how changes in hydrologic forcing, such as increasing amounts of
410 precipitation falling as rain rather than snow, will impact future watershed carbon fluxes. In this
411 context, shifts in streamwater $\delta^{18}O$ will allow its use as a proxy for hydrological and linked
412 ecosystem effects that can be expected to occur under projected climate change in the region
413 (Shanley et al. 2015).

414 There are thousands of streams in the Alaskan PCTR that drain into near-shore marine
415 ecosystems; many of them are poorly accessible for direct measurement and each has a different
416 mosaic of landscape features and contributing soils. Describing the linkages between landscape
417 cover, biomass and stream biogeochemistry is a critical step in understanding how changes in
418 climate and forest management may influence terrestrial and linked aquatic ecosystem processes.
419 Our finding that LiDAR generated data on watershed morphology and vegetation explained more
420 than 57% of the variation in concentration for all measured constituents except Mg^{2+}
421 demonstrates the potential for this high resolution landscape analysis to generate first order
422 estimates of stream DOM and nutrient export across the region. These findings provide evidence
423 for a biogeochemical division that exists within the Cowee Creek watershed where streams can
424 be organized by their dominant watershed characteristics (i.e. aboveground biomass, slope). We
425 suggest the use of LIDAR or other biomass quantification methodologies in many of the small
426 and remote watersheds across the Alaskan PCTR could help calibrate regional biogeochemical
427 flux models to predict the potential impacts of forest change and management activities on future
428 carbon and nutrient export to the Gulf of Alaska. With proper field calibration, this approach

could also be applied to other forested regions with high landscape heterogeneity and relatively small watersheds, such as the Pacific northwest of the U.S.A and southern Patagonia. This information could inform land management decisions that have the potential to alter ecosystems services related to watershed biogeochemical fluxes.

Acknowledgements

We thank John Krapek at University of Alaska Fairbanks for field assistance and Durelle Scott at Virginia Tech for laboratory analysis. This study was supported by an Alaska NASA EPSCoR grant to B.B. and the USDA Forest Service Pacific Northwest Research Station.

References

Ågren, A., Buffam, I., Jansson, M., and Laudon, H. 2007. Importance of seasonality and small streams for the landscape regulation of dissolved organic carbon export. Journal of Geophysical Research **112**(G3). doi:10.1029/2006JG000381.

Ågren, A.M., Buffam, I., Cooper, D.M., Tiwari, T., Evans, C.D., and Laudon, H. 2014. Can the heterogeneity in stream dissolved organic carbon be explained by contributing landscape elements? Biogeosciences **11**(4): 1199–1213. doi:10.5194/bg-11-1199-2014.

Brieman, L. 2001. Random Forest. Machine Learning **45**(1): 5–32.

Brieman, L., Friedman, J, Olshen, R, and Stone, C. 1984. Classification and Regression Trees. Wadsworth, Belmont, CA.

Brookshire, E.N.J., Valett, H.M., Thomas, S.A., and Webster, J.R. 2005. Coupled cycling of dissolved organic nitrogen and carbon in a forest stream. Ecology **86**(9): 2487–2496. doi:10.1890/04-1184.

450 Buma, B., and Johnson, A.C. 2015. The role of windstorm exposure and yellow cedar decline on
451 landslide susceptibility in southeast Alaskan temperate rainforests. Geomorphology **228**:
452 504–511. doi:10.1016/j.geomorph.2014.10.014.
453 Butman, D., Stackpoole, S., Stets, E., McDonald, C.P., Clow, D.W., and Striegl, R.G. 2016.
454 Aquatic carbon cycling in the conterminous United States and implications for terrestrial
455 carbon accounting. Proceedings of the National Academy of Sciences **113**(1): 58–63.
456 doi:10.1073/pnas.1512651112.
457 Clark, M.J., Cresser, M.S., Smart, R., Chapman, P.J., and Edwards, A.C. 2004. The influence of
458 catchment characteristics on the seasonality of carbon and nitrogen species
459 concentrations in upland rivers of Northern Scotland. Biogeochemistry **68**(1): 1–19.
460 doi:10.1023/B:BIOG.0000025733.07568.11.
461 Cleveland, C.C., Townsend, A.R., and Schmidt, S.K. 2002. Phosphorus Limitation of Microbial
462 Processes in Moist Tropical Forests: Evidence from Short-term Laboratory Incubations
463 and Field Studies. Ecosystems **5**(7): 0680–0691. doi:10.1007/s10021-002-0202-9.
464 Cole, J.J., Prairie, Y.T., Caraco, N.F., McDowell, W.H., Tranvik, L.J., Striegl, R.G., Duarte,
465 C.M., Kortelainen, P., Downing, J.A., Middelburg, J.J., and Melack, J. 2007. Plumbing
466 the Global Carbon Cycle: Integrating Inland Waters into the Terrestrial Carbon Budget.
467 Ecosystems **10**(1): 172–185. doi:10.1007/s10021-006-9013-8.
468 Compton, J.E., Church, M.R., Larned, S.T., and Hogsett, W.E. 2003. Nitrogen Export from
469 Forested Watersheds in the Oregon Coast Range: The Role of N 2 -fixing Red Alder.
470 Ecosystems **6**(8): 773–785. doi:10.1007/s10021-002-0207-4.
471 Creed, I.F., Beall, F.D., Clair, T.A., Dillon, P.J., and Hesslein, R.H. 2008. Predicting export of
472 dissolved organic carbon from forested catchments in glaciated landscapes with shallow

473 soils: A simple but robust DOC export model. Global Biogeochemical Cycles **22**(4): n/a–
474 n/a. doi:10.1029/2008GB003294.
475 Cuevas, J.G., Soto, D., Arismendi, I., Pino, M., Lara, A., and Oyarzún, C. 2006. Relating land
476 cover to stream properties in southern Chilean watersheds: trade-off between geographic
477 scale, sample size, and explicative power. Biogeochemistry **81**(3): 313–329.
478 doi:10.1007/s10533-006-9043-5.
479 Cutler, D.R., Edwards, T.C., Beard, K.H., Cutler, A., Hess, K.T., Gibson, J., and Lawler, J.J.
480 2007. Random forests for classification in ecology. Ecology **88**(11): 2783–2792.
481 doi:10.1890/07-0539.1.
482 D'Amore, D.V., Edwards, R.T., Herendeen, P.A., Hood, E., and Fellman, J.B. 2015. Dissolved
483 Organic Carbon Fluxes from Hydropedologic Units in Alaskan Coastal Temperate
484 Rainforest Watersheds. Soil Science Society of America Journal **79**(2): 378.
485 doi:10.2136/sssaj2014.09.0380.
486 D'Amore, D.V., Fellman, J.B., Edwards, R.T., and Hood, E. 2010. Controls on dissolved organic
487 matter concentrations in soils and streams from a forested wetland and sloping bog in
488 southeast Alaska. Ecohydrology **3**(3): 249–261. doi:10.1002/eco.101.
489 Dalzell, B.J., Filley, T.R., and Harbor, J.M. 2005. Flood pulse influences on terrestrial organic
490 matter export from an agricultural watershed. Journal of Geophysical Research **110**(G2).
491 doi:10.1029/2005JG000043.
492 Dansgaard, W. 1964. Stable isotopes in precipitation. Tellus **16**(4): 436–468. doi:10.1111/j.2153-
493 3490.1964.tb00181.x.

494 Dietermann, N., and Weiler, M. 2013. Spatial distribution of stable water isotopes in alpine snow
495 cover. Hydrology and Earth System Sciences **17**(7): 2657–2668. doi:10.5194/hess-17-
496 2657-2013.
497 Dillon, P.J., and Molot, L.A. 1997. Effect of landscape form on export of dissolved organic
498 carbon, iron, and phosphorus from forested stream catchments. Water Resources
499 Research **33**(11): 2591–2600. doi:10.1029/97WR01921.
500 Dogramaci, S., Skrzypek, G., Dodson, W., and Grierson, P.F. 2012. Stable isotope and
501 hydrochemical evolution of groundwater in the semi-arid Hamersley Basin of subtropical
502 northwest Australia. Journal of Hydrology **475**: 281–293.
503 doi:10.1016/j.jhydrol.2012.10.004.
504 Evans, C.D., Monteith, D.T., and Cooper, D.M. 2005. Long-term increases in surface water
505 dissolved organic carbon: Observations, possible causes and environmental impacts.
506 Environmental Pollution **137**(1): 55–71. doi:10.1016/j.envpol.2004.12.031.
507 Fellman, J.B., D'Amore, D.V., Hood, E., and Boone, R.D. 2008. Fluorescence characteristics
508 and biodegradability of dissolved organic matter in forest and wetland soils from coastal
509 temperate watersheds in southeast Alaska. Biogeochemistry **88**(2): 169–184.
510 doi:10.1007/s10533-008-9203-x.
511 Fellman, J.B., Hood, E., Edwards, R.T., and D'Amore, D.V. 2009. Changes in the concentration,
512 biodegradability, and fluorescent properties of dissolved organic matter during
513 stormflows in coastal temperate watersheds. Journal of Geophysical Research **114**(G1).
514 doi:10.1029/2008JG000790.
515 Fellman, J.B., Hood, E., Spencer, R.G.M., Stubbins, A., and Raymond, P.A. 2014a. Watershed
516 Glacier Coverage Influences Dissolved Organic Matter Biogeochemistry in Coastal

517 Watersheds of Southeast Alaska. Ecosystems **17**(6): 1014–1025. doi:10.1007/s10021-
518 014-9777-1.
519 Fellman, J.B., Nagorski, S., Pyare, S., Vermilyea, A.W., Scott, D., and Hood, E. 2014b. Stream
520 temperature response to variable glacier coverage in coastal watersheds of Southeast
521 Alaska. Hydrological Processes **28**(4): 2062–2073. doi:10.1002/hyp.9742.
522 Friedman, J. 1991. Multivariate Adaptive Regression Splines. The Annals of Statistics **19**(1): 1–
523 67.
524 Frost, P.C., Larson, J.H., Johnston, C.A., Young, K.C., Maurice, P.A., Lamberti, G.A., and
525 Bridgham, S.D. 2006. Landscape predictors of stream dissolved organic matter
526 concentration and physicochemistry in a Lake Superior river watershed. Aquatic Sciences
527 **68**(1): 40–51. doi:10.1007/s00027-005-0802-5.
528 Gergel, S.E., Turner, M.G., and Kratz, T.K. 1999. Dissolved organic carbon as an indicator of
529 the scale of watershed influence on lakes and rivers. Ecological Applications **9**(4): 1377–
530 1390. doi:10.1890/1051-0761(1999)009[1377:DOCAAI]2.0.CO;2.
531 Giesler, R., Satoh, F., Ilstedt, U., and Nordgren, A. 2004. Microbially Available Phosphorus in
532 Boreal Forests: Effects of Aluminum and Iron Accumulation in the Humus Layer.
533 Ecosystems **7**(2). doi:10.1007/s10021-003-0223-z.
534 Del Giorgio, P.A., and Pace, M.L. 2008. Relative independence of organic carbon transport and
535 processing in a large temperate river: The Hudson River as both pipe and reactor.
536 Limnology and Oceanography **53**(1): 185–197. doi:10.4319/lo.2008.53.1.0185.
537 Güneralp, İ., Filippi, A.M., and Randall, J. 2014. Estimation of floodplain aboveground biomass
538 using multispectral remote sensing and nonparametric modeling. International Journal of

539 Applied Earth Observation and Geoinformation **33**: 119–126.
540 doi:10.1016/j.jag.2014.05.004.
541 Hamilton, S.K., Bunn, S.E., Thoms, M.C., and Marshall, J.C. 2005. Persistence of aquatic
542 refugia between flow pulses in a dryland river system (Cooper Creek, Australia).
543 Limnology and Oceanography **50**(3): 743–754. doi:10.4319/lo.2005.50.3.0743.
544 Hanley, K.W., Wollheim, W.M., Salisbury, J., Huntington, T., and Aiken, G. 2013. Controls on
545 dissolved organic carbon quantity and chemical character in temperate rivers of North
546 America: Controls on DOC in North American rivers. Global Biogeochemical Cycles
547 **27**(2): 492–504. doi:10.1002/gbc.20044.
548 Harmon, M., Woodall, C., Fasth, B., Sexton, J., and Yatkov, M. 2011. Differences between
549 standing and downed dead tree wood density reduction factors: A comparison across
550 decay classes and tree species. USDA Forest Service Research Paper NRS-15.
551 Heath, L.S., Smith, J.E., Woodall, C.W., Azuma, D.L., and Waddell, K.L. 2011. Carbon stocks
552 on forestland of the United States, with emphasis on USDA Forest Service ownership.
553 Ecosphere **2**(1): art6. doi:10.1890/ES10-00126.1.
554 Hudak, A.T., Strand, E.K., Vierling, L.A., Byrne, J.C., Eitel, J.U.H., Martinuzzi, S., and
555 Falkowski, M.J. 2012. Quantifying aboveground forest carbon pools and fluxes from
556 repeat LiDAR surveys. Remote Sensing of Environment **123**: 25–40.
557 doi:10.1016/j.rse.2012.02.023.
558 Jankowski, K., Schindler, D.E., and Lisi, P.J. 2014. Temperature sensitivity of community
559 respiration rates in streams is associated with watershed geomorphic features. Ecology
560 **95**(10): 2707–2714. doi:10.1890/14-0608.1.

561 Johnson, K.D., Harden, J., McGuire, A.D., Bliss, N.B., Bockheim, J.G., Clark, M., Nettleton-
562 Hollingsworth, T., Jorgenson, M.T., Kane, E.S., Mack, M., O'Donnell, J., Ping, C.-L.,
563 Schuur, E.A.G., Turetsky, M.R., and Valentine, D.W. 2011. Soil carbon distribution in
564 Alaska in relation to soil-forming factors. Geoderma **167-168**: 71–84.
565 doi:10.1016/j.geoderma.2011.10.006.
566 Kaplan, L.A., and Bott, T.L. 1985. Acclimation of stream-bed heterotrophic microflora:
567 metabolic responses to dissolved organic matter. Freshwater Biology **15**(4): 479–492.
568 doi:10.1111/j.1365-2427.1985.tb00218.x.
569 Kaplan, L.A., Newbold, J.D., Horn, D.J.V., Dow, C.L., Aufdenkampe, A.K., and Jackson, J.K.
570 2006. Organic matter transport in New York City drinking-water-supply watersheds.
571 Journal of the North American Benthological Society **25**(4): 912–927. doi:10.1899/0887-
572 3593(2006)025[0912:OMTINY]2.0.CO;2.
573 Keyser, C.E. 2008. Southeast Alaska and Coastal British Columbia (AK) Variant Overview –
574 Forest Vegetation Simulator. Internal Rep. Fort Collins, CO: U. S. Department of
575 Agriculture, Forest Service, Forest Management Service Center.
576 Kothawala, D.N., Stedmon, C.A., Müller, R.A., Weyhenmeyer, G.A., Köhler, S.J., and Tranvik,
577 L.J. 2014. Controls of dissolved organic matter quality: evidence from a large-scale
578 boreal lake survey. Global Change Biology **20**(4): 1101–1114. doi:10.1111/gcb.12488.
579 Kozak, A., Munro, D.D., and Smith, J.H.G. 1969. Taper Functions and their Application in
580 Forest Inventory. The Forestry Chronicle **45**(4): 278–283. doi:10.5558/tfc45278-4.
581 Lapierre, J.-F., Guillemette, F., Berggren, M., and del Giorgio, P.A. 2013. Increases in
582 terrestrially derived carbon stimulate organic carbon processing and CO2 emissions in
583 boreal aquatic ecosystems. Nature Communications **4**. doi:10.1038/ncomms3972.

584 Lidman, F., Köhler, S.J., Mörth, C.-M., and Laudon, H. 2014. Metal Transport in the Boreal
585 Landscape—The Role of Wetlands and the Affinity for Organic Matter. Environmental
586 Science & Technology **48**(7): 3783–3790. doi:10.1021/es4045506.
587 Mattsson, T., Kortelainen, P., and Räike, A. 2005. Export of DOM from Boreal Catchments:
588 Impacts of Land Use Cover and Climate. Biogeochemistry **76**(2): 373–394.
589 doi:10.1007/s10533-005-6897-x.
590 Miller, M.P. 2012. The influence of reservoirs, climate, land use and hydrologic conditions on
591 loads and chemical quality of dissolved organic carbon in the Colorado River. Water
592 Resources Research **48**(12): n/a–n/a. doi:10.1029/2012WR012312.
593 Moore, S., Evans, C.D., Page, S.E., Garnett, M.H., Jones, T.G., Freeman, C., Hooijer, A.,
594 Wiltshire, A.J., Limin, S.H., and Gauci, V. 2013. Deep instability of deforested tropical
595 peatlands revealed by fluvial organic carbon fluxes. Nature **493**(7434): 660–663.
596 doi:10.1038/nature11818.
597 Murphy, J., and Riley, J.P. 1962. A modified single solution method for the determination of
598 phosphate in natural waters. Analytica Chimica Acta **27**: 31–36. doi:10.1016/S0003-
599 2670(00)88444-5.
600 Olander, L., and Vitousek, P. 2005. Short-term controls over inorganic phosphorus during soil
601 and ecosystem development. Soil Biology and Biochemistry **37**(4): 651–659.
602 doi:10.1016/j.soilbio.2004.08.022.
603 Oyarzún, C.E., Godoy, R., De Schrijver, A., Staelens, J., and Lust, N. 2005. Water chemistry and
604 nutrient budgets in an undisturbed evergreen rainforest of Southern Chile.
605 Biogeochemistry **71**(1): 107–123. doi:10.1007/s10533-005-4107-5.

606 Paul, D., Skrzypek, G., and Fórizs, I. 2007. Normalization of measured stable isotopic
607 compositions to isotope reference scales – a review. Rapid Communications in Mass
608 Spectrometry **21**(18): 3006–3014. doi:10.1002/rcm.3185.
609 Pellerin, B.A., Wollheim, W.M., Hopkinson, C.S., McDowell, W.H., Williams, M.R.,
610 Vörösmarty, C.J., and Daley, M.L. 2004. Role of wetlands and developed land use on
611 dissolved organic nitrogen concentrations and DON/TDN in northeastern U.S. rivers and
612 streams. Limnology and Oceanography **49**(4): 910–918. doi:10.4319/lo.2004.49.4.0910.
613 Petrone, K.C. 2010. Catchment export of carbon, nitrogen, and phosphorus across an agro-urban
614 land use gradient, Swan-Canning River system, southwestern Australia. Journal of
615 Geophysical Research **115**(G1). doi:10.1029/2009JG001051.
616 Porder, S., Paytan, A., and Vitousek, P.M. 2005. Erosion and landscape development affect plant
617 nutrient status in the Hawaiian Islands. Oecologia **142**(3): 440–449. doi:10.1007/s00442-
618 004-1743-8.
619 Qualls, R.G. 2000. Comparison of the behavior of soluble organic and inorganic nutrients in
620 forest soils. Forest Ecology and Management **138**(1-3): 29–50. doi:10.1016/S0378-
621 1127(00)00410-2.
622 Qualls, R.G., and Haines, B.L. 1992. Biodegradability of Dissolved Organic Matter in Forest
623 Throughfall, Soil Solution, and Stream Water. Soil Science Society of America Journal
624 **56**(2): 578. doi:10.2136/sssaj1992.03615995005600020038x.
625 Qualls, R.G., and Richardson, C.J. 2003. Factors controlling concentration, export, and
626 decomposition of dissolved organic nutrients in the Everglades of Florida.
627 Biogeochemistry **62**(2): 197–229.

628 Räike, A., Kortelainen, P., Mattsson, T., and Thomas, D.N. 2015. Long-term trends (1975–2014)
629 in the concentrations and export of carbon from Finnish rivers to the Baltic Sea: organic
630 and inorganic components compared. Aquatic Sciences. doi:10.1007/s00027-015-0451-2.
631 Rasmussen, J.B., Godbout, L., and Schallenberg, M. 1989. The humic content of lake water and
632 its relationship to watershed and lake morphometry. Limnology and Oceanography **34**(7):
633 1336–1343. doi:10.4319/lo.1989.34.7.1336.
634 Regnier, P., Friedlingstein, P., Ciais, P., Mackenzie, F.T., Gruber, N., Janssens, I.A., Laruelle,
635 G.G., Lauerwald, R., Luyssaert, S., Andersson, A.J., Arndt, S., Arnosti, C., Borges, A.V.,
636 Dale, A.W., Gallego-Sala, A., Goddéris, Y., Goossens, N., Hartmann, J., Heinze, C.,
637 Ilyina, T., Joos, F., LaRowe, D.E., Leifeld, J., Meysman, F.J.R., Munhoven, G.,
638 Raymond, P.A., Spahni, R., Suntharalingam, P., and Thullner, M. 2013. Anthropogenic
639 perturbation of the carbon fluxes from land to ocean. Nature Geoscience **6**(8): 597–607.
640 doi:10.1038/ngeo1830.
641 Shanley, C.S., Pyare, S., Goldstein, M.I., Alaback, P.B., Albert, D.M., Beier, C.M., Brinkman,
642 T.J., Edwards, R.T., Hood, E., MacKinnon, A., McPhee, M.V., Patterson, T.M., Suring,
643 L.H., Tallmon, D.A., and Wipfli, M.S. 2015. Climate change implications in the northern
644 coastal temperate rainforest of North America. Climatic Change **130**: 155–170.
645 doi:10.1007/s10584-015-1355-9.
646 Simon, K.S., Townsend, C.R., Biggs, B.J.F., and Bowden, W.B. 2005. Temporal variation of N
647 and P uptake in 2 New Zealand streams. Journal of the North American Benthological
648 Society **24**(1): 1–18. doi:10.1899/0887-3593(2005)024<0001:TVONAP>2.0.CO;2.

649 Sørensen, R., Zinko, U., and Seibert, J. 2006. On the calculation of the topographic wetness
650 index: evaluation of different methods based on field observations. Hydrology and Earth
651 System Sciences **10**(1): 101–112. doi:10.5194/hess-10-101-2006.
652 Standish, J., Manning, G., and Demaerschalk, J. 1985. Development of biomass equations for
653 British Columbia tree species (No. BC-X-264).
654 Stanley, E.H., and Maxted, J.T. 2008. Changes in the dissolved nitrogen pool across land cover
655 gradients in Wisconsin streams. Ecological Applications **18**(7): 1579–1590.
656 doi:10.1890/07-1379.1.
657 Striegl, R.G., Aiken, G.R., Dornblaser, M.M., Raymond, P.A., and Wickland, K.P. 2005. A
658 decrease in discharge-normalized DOC export by the Yukon River during summer
659 through autumn. Geophysical Research Letters **32**(21). doi:10.1029/2005GL024413.
660 Tank, S.E., Raymond, P.A., Striegl, R.G., McClelland, J.W., Holmes, R.M., Fiske, G.J., and
661 Peterson, B.J. 2012. A land-to-ocean perspective on the magnitude, source and
662 implication of DIC flux from major Arctic rivers to the Arctic Ocean: Arctic river DIC.
663 Global Biogeochemical Cycles **26**(4): n/a–n/a. doi:10.1029/2011GB004192.
664 Ter-Mikaelian, M.T., and Korzukhin, M.D. 1997. Biomass equations for sixty-five North
665 American tree species. Forest Ecology and Management **97**(1): 1–24. doi:10.1016/S0378-
666 1127(97)00019-4.
667 Valderrama, J.C. 1981. The simultaneous analysis of total nitrogen and total phosphorus in
668 natural waters. Marine Chemistry **10**(2): 109–122. doi:10.1016/0304-4203(81)90027-X.
669 Vitousek, P., Chadwick, O., Matson, P., Allison, S., Derry, L., Kettley, L., Luers, A., Mecking,
670 E., Monastra, V., and Porder, S. 2003. Erosion and the Rejuvenation of Weathering-

671 derived Nutrient Supply in an Old Tropical Landscape. Ecosystems **6**(8): 762–772.
672 doi:10.1007/s10021-003-0199-8.
673 Vitousek, P.M. 1977. The Regulation of Element Concentrations in Mountain Streams in the
674 Northeastern United States. Ecological Monographs **47**(1): 65. doi:10.2307/1942224.
675 Vitousek, P.M. 1982. Nutrient Cycling and Nutrient Use Efficiency. The American Naturalist
676 **119**(4): 553–572.
677 Vitvar, T., and Balderer, W. 1997. Estimation of mean water residence times and runoff
678 generation by180 measurements in a Pre-Alpine catchment (Rietholzbach, Eastern
679 Switzerland). Applied Geochemistry **12**(6): 787–796. doi:10.1016/S0883-
680 2927(97)00045-0.
681 Weishaar, J.L., Aiken, G.R., Bergamaschi, B.A., Fram, M.S., Fujii, R., and Mopper, K. 2003.
682 Evaluation of Specific Ultraviolet Absorbance as an Indicator of the Chemical
683 Composition and Reactivity of Dissolved Organic Carbon. Environmental Science &
684 Technology **37**(20): 4702–4708. doi:10.1021/es030360x.
685 Wiegner, T.N., Kaplan, L.A., Newbold, J.D., and Ostrom, P.H. 2005. Contribution of dissolved
686 organic C to stream metabolism: a mesocosm study using 13C-enriched tree-tissue
687 leachate. Journal of the North American Benthological Society **24**(1): 48–67.
688 doi:10.1899/0887-3593(2005)024<0048:CODOCT>2.0.CO;2.
689 Wigington, P.J., Church, M.R., Strickland, T.C., Eshleman, K.N., and Sickle, J.V. 1998. Autumn
690 chemistry of Oregon coast range streams. Journal of the American Water Resources
691 Association **34**(5): 1035–1049. doi:10.1111/j.1752-1688.1998.tb04152.x.
692 Williams, C.J., Yamashita, Y., Wilson, H.F., Jaffé, R., and Xenopoulos, M.A. 2010. Unraveling
693 the role of land use and microbial activity in shaping dissolved organic matter

694 characteristics in stream ecosystems. Limnology and Oceanography **55**(3): 1159–1171.
695 doi:10.4319/lo.2010.55.3.1159.
696

697 Table 1. Mean watershed characteristics and biogeochemical concentrations for our 37 study
698 streams.

	Minimum	Maximum	Mean	SD
Size (Ha)	0.75	597.2	49.3	127.8
Slope (º)	9.5	35.3	23.7	7.1
Elevation (m)	119.0	1008.8	439.6	215.3
Aboveground biomass (Mg ha^{-1})	71.7	652.8	367.3	186.9
TWI	7.9	9.5	8.7	0.4
Stream temperature (ºC)	3.2	84.2	15.8	19.0
Specific conductivity (µs cm^{-1})	5.1	13.8	9.7	1.6
$\delta^{18}O$ (‰)	-10.2	-14.4	-12.5	0.8
DOC (mg C L^{-1})	0.41	30.48	5.73	6.09
DON (mg N L^{-1})	<0.01	0.42	0.11	0.10
$SUVA_{254}$ (mg-C^{-1} m^{-1})	2.95	4.69	3.94	0.54
BDOC (mg C L^{-1})	0.07	4.98	0.87	1.13
DIN (mg N L^{-1})	BD	0.19	0.02	0.04
SRP (µg N L^{-1})	BD	17.41	1.86	2.87
TP (µg N L^{-1})	11.74	33.27	19.74	4.74
Ca^{2+} (mg C L^{-1})	BD	14.43	3.97	3.49
Mg^{2+} (mg C L^{-1})	BD	1.46	0.41	0.35
K^{+} (mg C L^{-1})	BD	0.59	0.12	0.13

699 BD corresponds to below detection limit. TWI corresponds to topographic wetness index.
700

Figure legends

Figure 1. Map of the study watersheds and stream sampling sites (yellow circles) near Juneau, southeast Alaska.

Figure 2. Random forest/CART tree and Box-whisker plots for $\delta^{18}O$ values (‰) across the 37 study streams.

Figure 3. Random forest/CART tree and Box-whisker plots for concentrations of a) DOC (mg C L^{-1}) and b) DON (mg N L^{-1}) across the 37 study streams.

Figure 4. Random forest/CART tree and Box-whisker plots for a) $SUVA_{254}$ values (L mg-C^{-1} m^{-1}) and b) bioavailable DOC (BDOC) concentrations (mg C L^{-1}) across the 37 study streams.

Figure 5. Random forest/CART tree and Box-whisker plots for concentrations (µg P L^{-1}) of a) soluble reactive P (SRP) and b) total P (TP) across the 37 study streams.

Figure 6. Random forest/CART tree and Box-whisker plots for concentrations (mg N L^{-1}) of dissolved inorganic N (DIN) across the 37 study streams.

Figure 7. Random forest/CART tree and Box-whisker plots for concentrations (mg L^{-1}) of Ca^{2+} across the 37 study streams.

Figure 8. Random forest/CART tree and Box-whisker plots for concentrations (mg L^{-1}) of a) K^{+} and b) Mg^{2+} across the 37 study streams.

719 Figure 1.
720

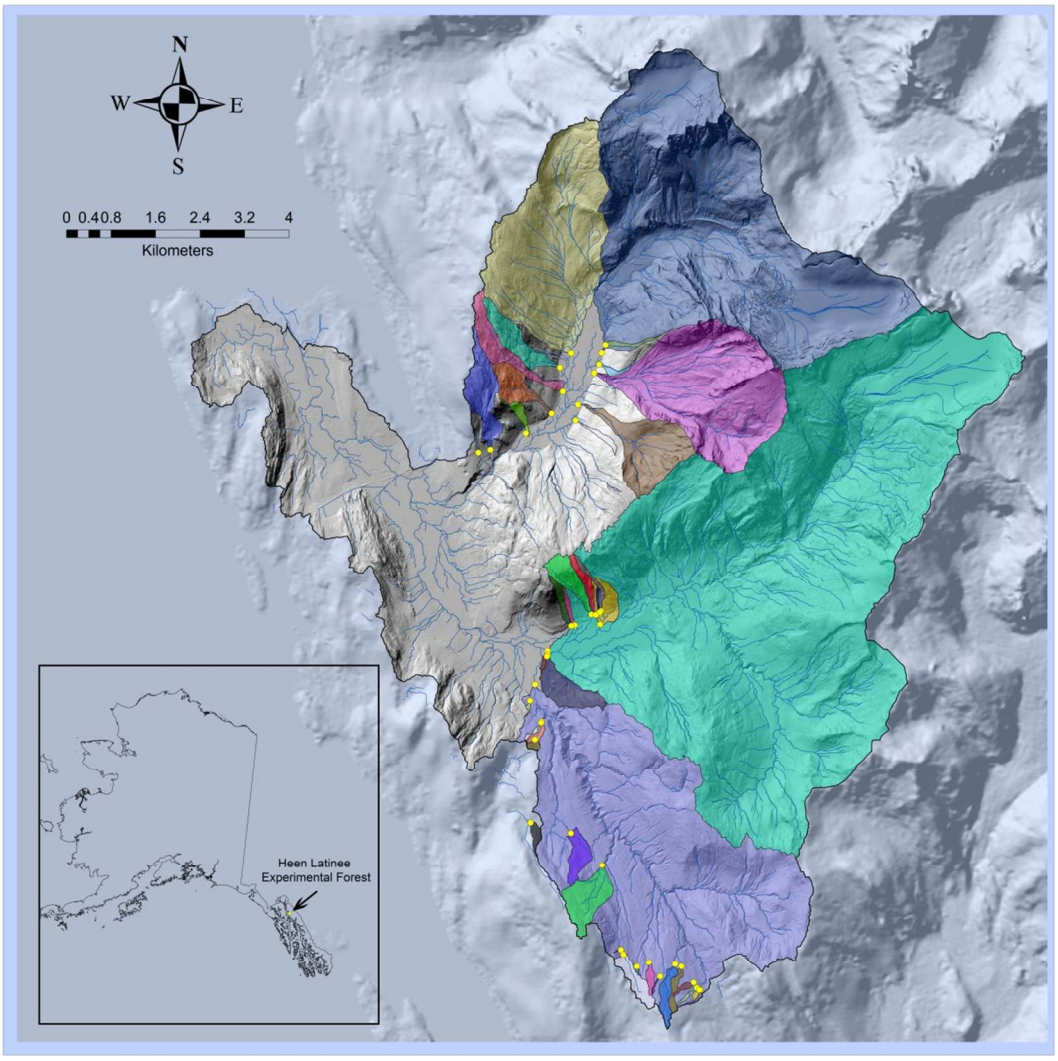

721
722

723 Figure 2.
724

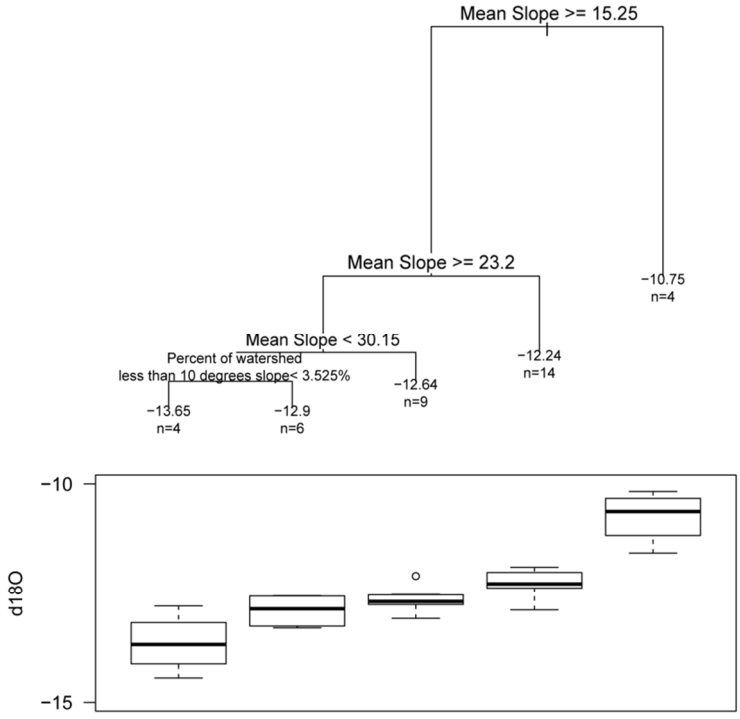

725
726
727
728

729 Figure 3.

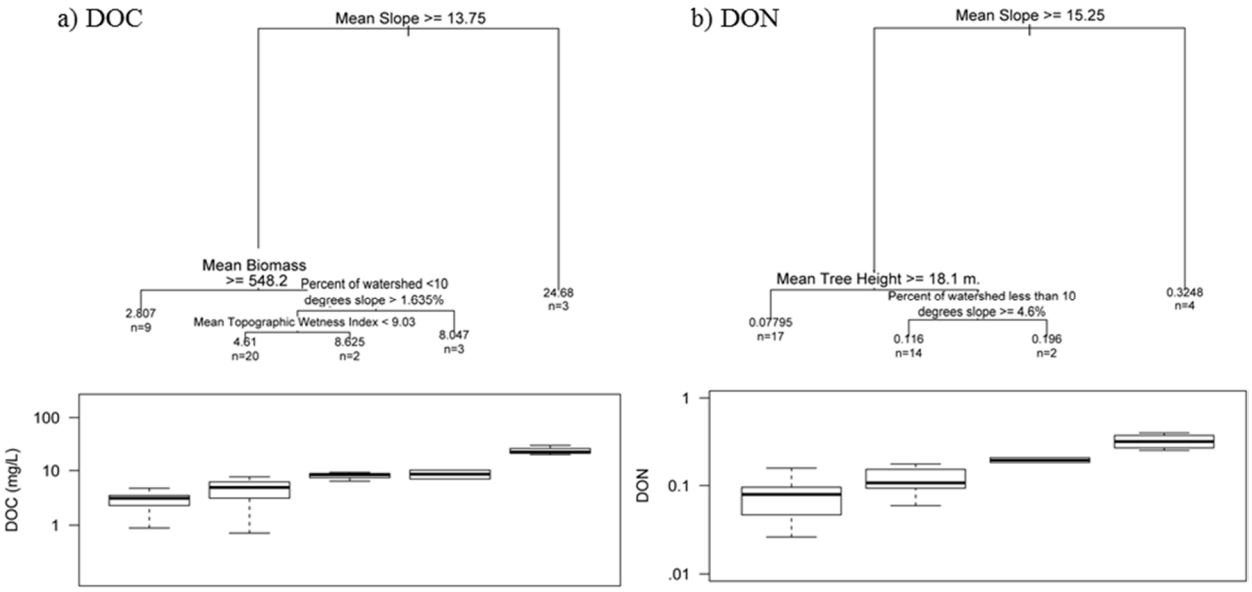

730
731
732

733 Figure 4.

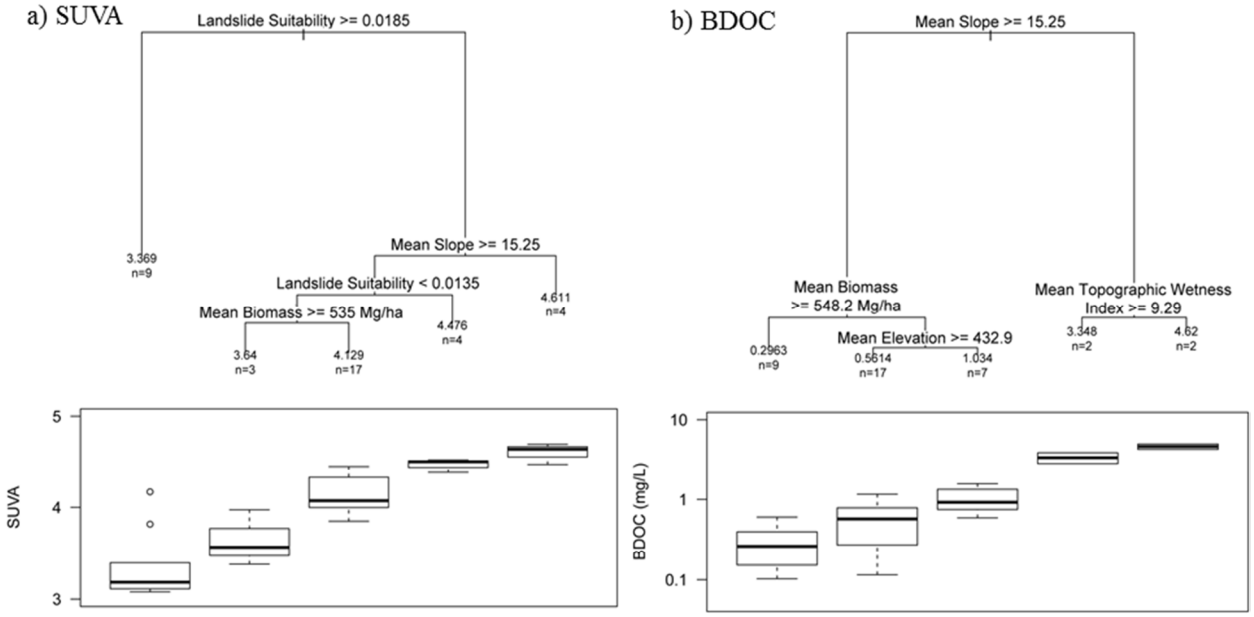

734
735

736 Figure 5.

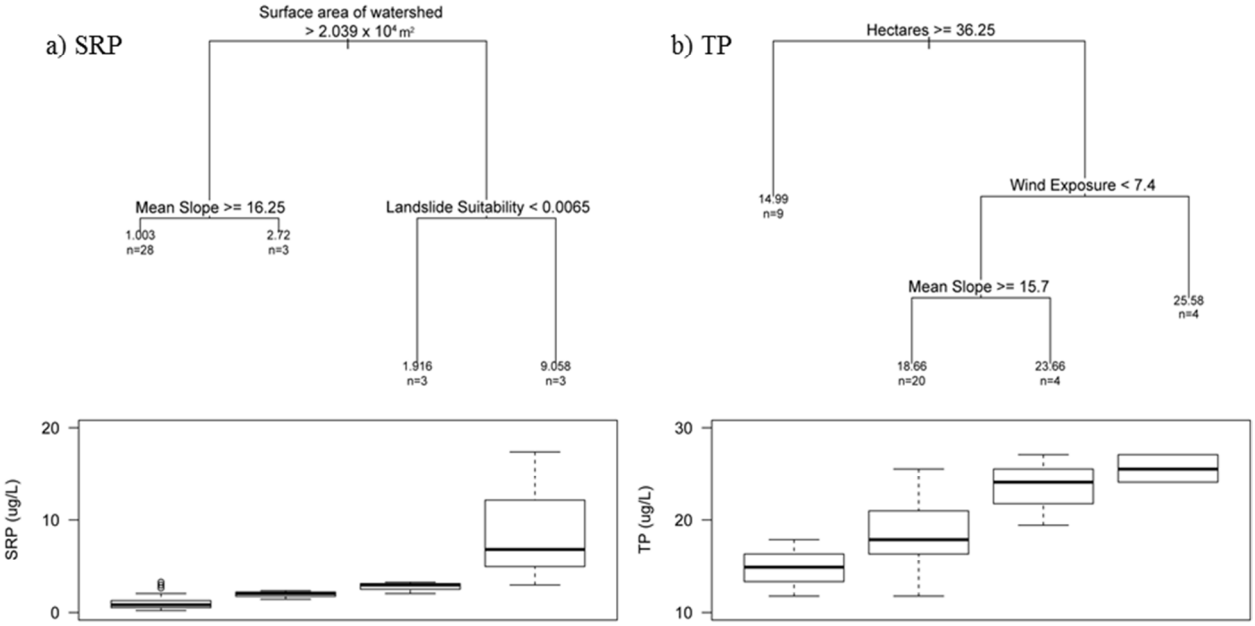

737
738

739 Figure 6.
740

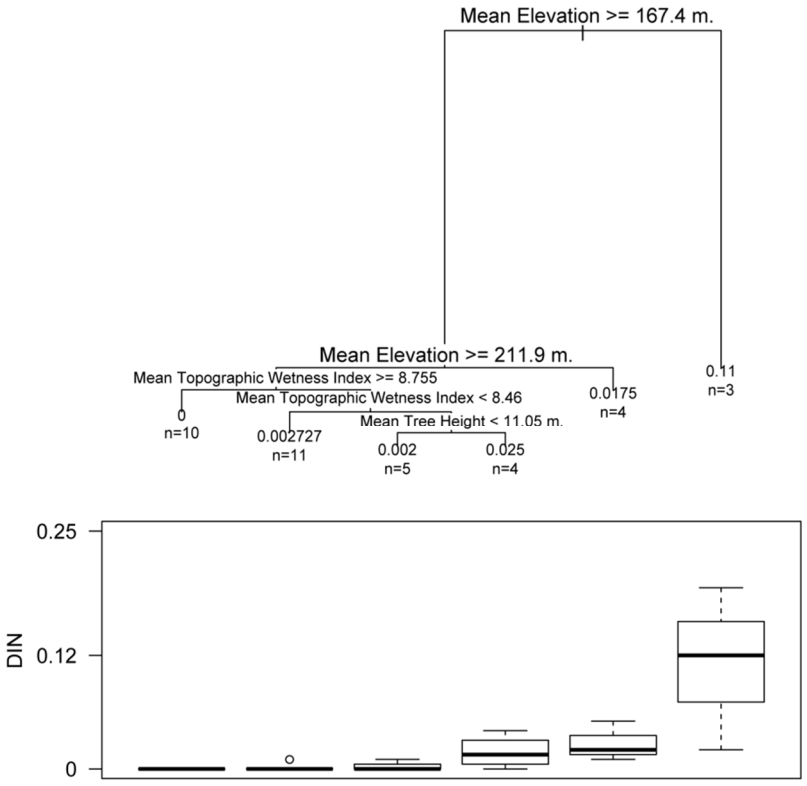

741
742

743 Figure 7.

744

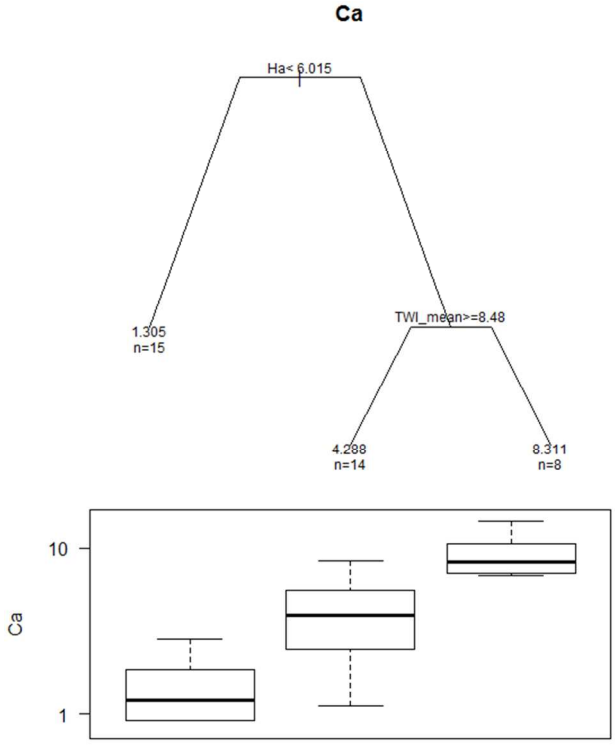

745

746

747

748 Figure 8.
749

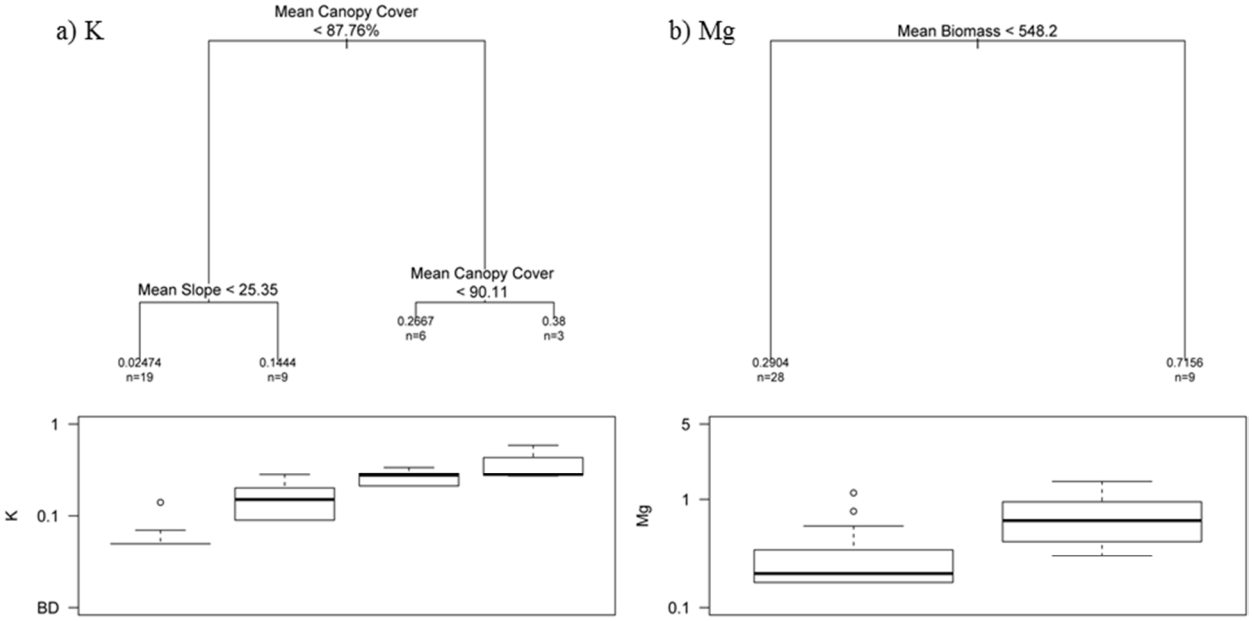

750
751